VICTORIA UNIVERSITY
MELBOURNE AUSTRALIA

Analysing steps in modelled global surface air temperature

Roger N Jones and James H Ricketts

Climate Change Working Paper 35

Victoria Institute of Strategic Economic Studies

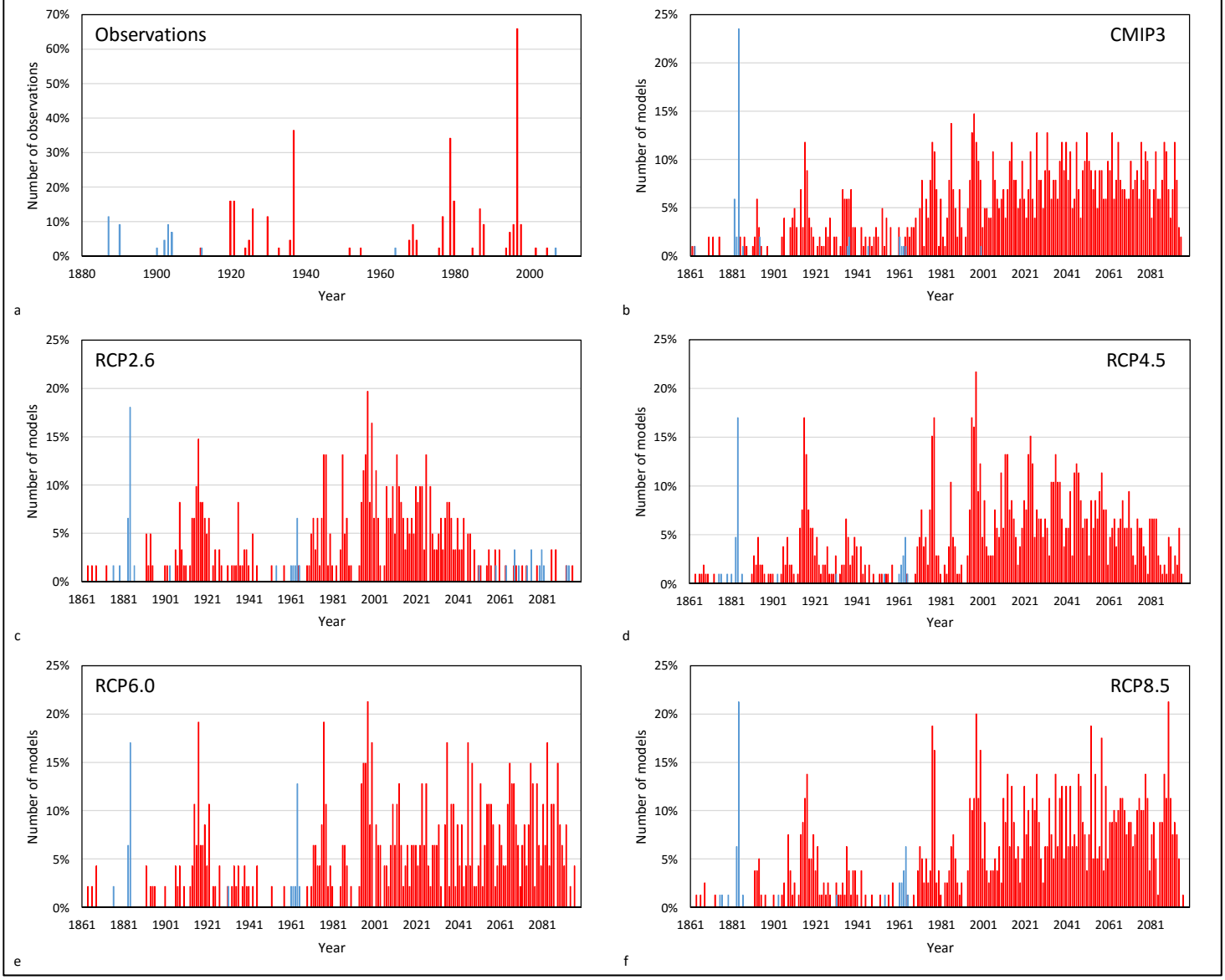

Key words: air temperature, global warming, decadal variability, climate change, climate modelling, step change

Acknowledgements

JR is the holder of a Victoria University posgraduate research scholarship. CMIP3 and CMIP5 archives are made available by the modeling groups, the Program for Climate Model Diagnosis and Intercomparison (PCMDI) and the WCRP's Working Group on Coupled Modelling (WGCM). The U.S. Department of Energy's Program for Climate Model Diagnosis and Intercomparison provides coordinating support and led development of software infrastructure in partnership with the Global Organization for Earth System Science Portals. Useful discussions were held with Celeste Young, Peter Sheehan, Roger Bodman, Penny Whetton, Kevin Hennessy, Kris Ebi, Ben Preston, Jim Bowler, Rod Marsh and the big shift group. D Kelly O'Day for the programming and macros adapted to conduct multiple trend analysis and graphics. Roger Bodman reviewed the manuscript.

Suggested citation

Jones, R.N. and Ricketts, J.H. (2015) Analysing steps in modelled global surface air temperature. Climate Change Working Paper No. 35, Victoria Institute of Strategic Economic Studies, Victoria University, Melbourne, Australia.

Publishing Notes

This paper and a companion paper have been merged and added to and now are part of the paper Reconciling the signal and noise of atmospheric warming on decadal timescales, Climate Change Working Paper. No. 38.

ISBN: 978-1-86272-723-6

Victoria Institute of Strategic Economic Studies
Victoria University
Po Box 14428 Melbourne
Victoria Australia 8001
Phone +613 9919 1340
Fax +613 9919 1350
vises@vu.edu.au

Abstract

Here, we apply a multi-step bivariate test to detect shifts in modelled global surface air temperature to see whether historical simulations match the pattern of shifts in observations, assess so-called 'hiatus' periods between shifts and investigate the evolution of steps and trends under different emissions pathways. Key findings include: simulations reproduce the broad pattern of historical steps reasonably well, the 1996–2005 decade including the large 1996–98 step change, and total warming to 2005 shows no relationship with model equilibrium climate sensitivity (ECS). Nor does 20th century warming show any relationship with 21st century warming. Fifty-five percent of models produce a step change in 1996–98, and are followed by 'hiatus' periods of 7–26 years, eight being equal to or greater than the current 18 years. For the representation concentration pathway RCP4.6 multi-model ensemble (MME), total step changes 2006–95 are 3.5 times as effective in explaining total warming and climate sensitivity than internal trends. Under the lower RCP2.6 pathway, the MME stabilises around 2050 and the timing of stabilisation is dominated by climate variability rather than ECS. The finding that warming in both models and observations is dominated by shifts shows that the current emphasis on trend analysis alone is inadequate for analysing climate change. This has substantial implications for how climate risk is framed, analysed and communicated.

Introduction

A major gap in understanding the physical process of climate change, is how climate changes over decadal timescales (Solomon et al., 2011). This is very important information for managing future climate risks. The scientific literature contains two competing hypotheses linking anthropogenic climate change and variability(Corti et al., 1999;Hasselmann, 2002):

1. Anthropogenic climate change occurs independently of climate variability (*H1*).
2. Anthropogenic climate change interacts with climate variability (*H2*).

H1 is generally interpreted as a monotonic trend driven by gradual climate forcing that is mediated by climate variability (Swanson et al., 2009;Rahmstorf et al., 2012;Zhou and Tung, 2013), producing a straight line or curve with fluctuations around the trend. This is interpreted as a signal-to noise model where variations away from the trend are caused by the noise of climate variability (North et al., 1995;Hegerl and Zwiers, 2011;Santer et al., 2011). Physically, this describes climate change as a gradual process. In this model, decadal climate variability manifesting as regime shifts is assumed to imprint on long-term trends as changes in the rate of trend. This conceptual model dominates how climate change is analysed and communicated.

H2 describes interactions of climate change and variability that produce significant non-linear responses (Corti et al., 1999;Solomon et al., 2011;Kirtman et al., 2013). In this formulation, the signal, expressed in terms of key variables such as temperature, is non-linear. The main problem in detecting and attributing possible nonlinear signals has been a robust method for doing so (Rodionov, 2005;Reeves et al., 2007;Overland et al., 2008). Accordingly, we have developed a multi-step bivariate test based on the bivariate test of Maronna and Yohai (1978). Using that test, a companion paper (Jones and Ricketts, 2015) presents an analysis of step changes in observed mean regional and global air temperature, henceforth JR2015.

This paper undertakes a related analysis for simulated mean global surface temperature from the CMIP3 and CMIP5 climate model archives. The analysis is carried out in two parts. The first part investigates simulated 20th century temperatures to determine how well the models reproduce the pattern of step changes in the observed data. Special attention is paid to the so-called 'hiatus' period that followed the 1997 step change revealed in JR2015. The second part analyses how step changes evolve over the 21st century under the different Radiative Concentration Pathways (RCPs).

Method

Step changes are analysed using the Maronna-Yohai (1978) bivariate test using a slightly amended formulation of Bücher and Dessens (1991). It tests a single serially-independent variate (x^i) against a reference variate (y^i) using a random time series following Vivès and Jones (2005). The important outputs of the test in a time series of length N are, (1) The T_i statistic which is defined for times i <N, (2) the T_{i0} value which is the maximum T_i value, (3) i_0, the time associated with T_{i0}, (4) shift at that time, and (5) p, the probability of zero shift. Note that i_0 is the last year prior to the change.

The bivariate test has been used to detect inhomogeneities in single climate variables (Potter, 1981;Bücher and Dessens, 1991;Kirono and Jones, 2007;Sahin and Cigizoglu, 2010) and systematic regional shifts in a wide range of climatic time series (Buishand, 1984;Gan, 1995;Vivès and Jones, 2005;Jones, 2012). The test has been modified to account for multiple step changes against a null (random) time series, selecting the least number of steps within the allocated rules. A run of an analysis of a single time series consists of a screening pass, followed by 100 convergent passes. In both runs, since the reference variate is a flat random sequence, the reference is resampled each pass.

The procedure undertakes 100 trials, starting from the most significant shift in a time series (with each segment also being tested against the random reference 100 times) and, if p<0.01, will segment the series into shorter time series, repeating the process until a stable set of step changes is produced (see Supplementary Information JR2015 for specific rules). This process will select zero (if no significant shift) to several stable configurations. A stable set of results will produce 100 identical solutions and less stable results will produce two or more alternatives. The most frequent configuration is selected as the most stable.
Model data is sourced from the Climate Model Intercomparison Projects CMIP3 and CMIP5. Further details are contained in the Supplementary Information below.

Results

20th Century simulations (1861–2014)

JR2015 tested mean annual global surface air temperature anomalies from five groups, hemispheric temperatures from three groups and zonal temperatures from two groups. The percentage of annual statistically significant (p<0.01) shifts in all 44 time series of mean annual surface temperature of global to zonal scale covering 1880–2014, are shown in Figure 1a. For the five global temperature records tested, the years of change and number of records (positive unless indicated), are 1902 (1 negative), 1920 (2), 1921 (1), 1930 (2), 1937 (3), 1979 (1), 1980 (4) and 1997 (5). Another important shift date is 1986/87, which features in the northern hemisphere and global ocean sea surface temperature. Globally, this date produces shifts at p<0.05 for annual temperature and p<0.01 for quarterly anomalies using both the bivariate and t-test (Figure 3, JR2015). Two-thirds of all historical records shift in 1997 and one-third in 1980 and 1937. Lesser peaks of 10–15% occur in 1920, 1921, 1926, 1930, 1968–69, 1987 and 1988. The three shifts in 1979/80, 1986/87 and 1997/98 are the main reason for the higher rate of trend noted from around 1970.

Figure 1b shows step changes from the CMIP3 combined SRES scenarios A1B and A2 simulations for the 20th and 21st century, and Figures 1c–f CMIP5 show RCP2.6, RCP4.5, RCP 6.0 and RCP 8.5, respectively. The CMIP3 models were driven by observed forcing to 1999–2000 and do a reasonable job of capturing the three main post 1950 peaks. Not all the 102 CMIP3 20th century runs are independent, with the total including 14 ensemble averages (Supplementary Table 1). The CMIP5 models were driven by observed forcing to 2005 and reproduce the overall observed pattern more closely, with a better representation of the observed peaks and troughs. This may be due to improved representation of both natural and human-induced forcing as inputs, and to factors such as model resolution and improved representation of physical processes.

The RCP4.5 data set (Figure 1d) with 107 independent members, is the largest multi-model ensemble (MME; Supplementary Table 2). The three major post-1950 step changes are widely reproduced: 55% (58 of 107) of the runs undergo a step change in 1996–98 (17% step in 1996, 16% in 1997 and 22% in 1998), 40% of the runs

in 1976–78 and 19% in 1986–88. Of the pre-1950 peaks, the models peak around 1916, rather than 1920, and 1936–37 forms a minor peak, less prominent than in the observations. The volcanic eruptions of Krakatoa (1883) and Mt Agung (1963) both feature in the model simulations but less so in the observations. The mid-20th century period of little change is also reasonably well reproduced.

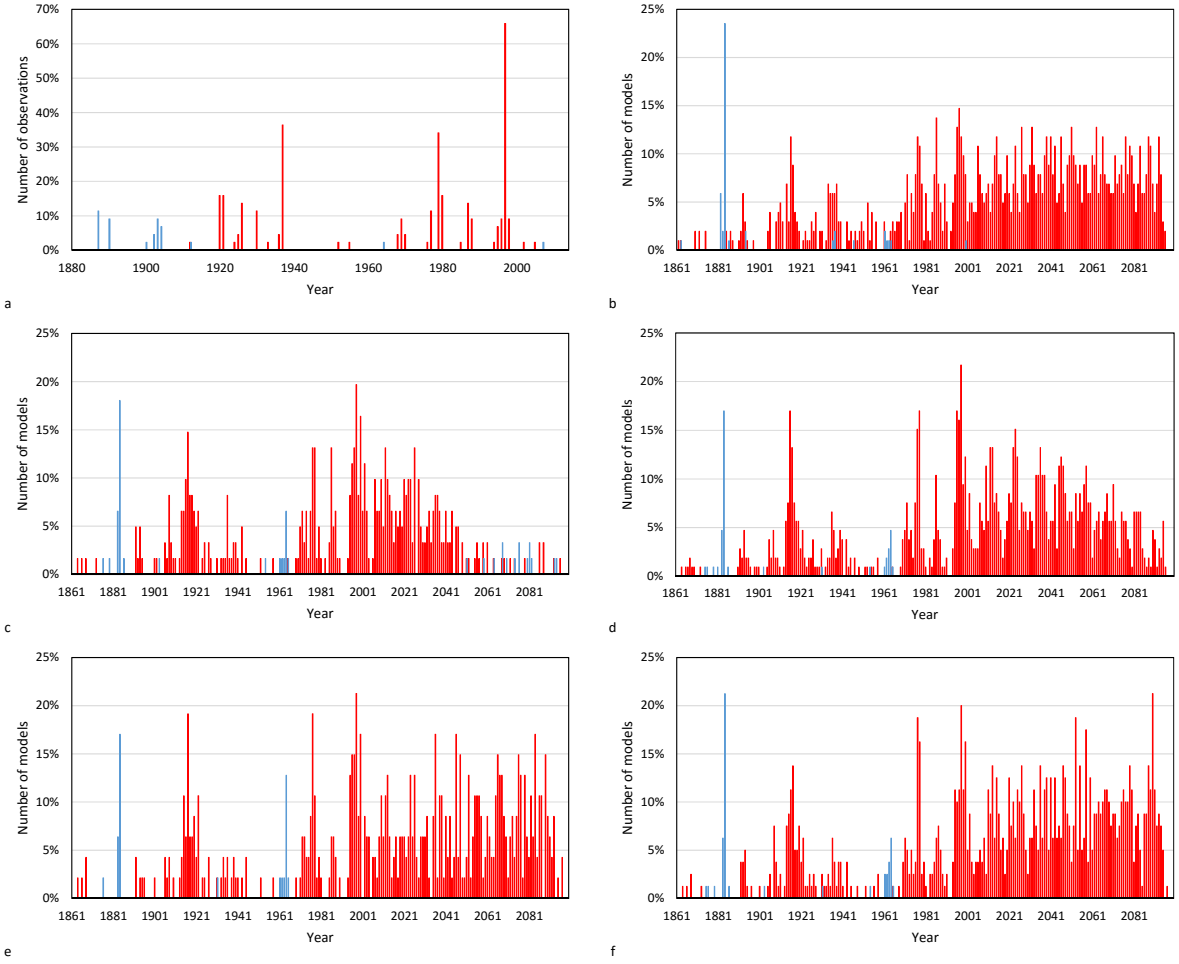

Figure 1. Step changes in observed and simulated surface air temperatures. Frequency in percent of statistically significant step changes from a) global, hemispheric and zonal averages (44 in total, 1880–2014); b) global mean warming from 102 model simulations from the CMIP3 archive for SRESA1b and A2 emission scenarios; c–f) global mean warming 1961–2100 from the CMIP5 archive for the c) RCP2.6 pathway (61), d) RCP4.5 pathway (107), e) RCP6.0 pathway (47) and f) RCP8.5 pathway (80).

The delayed peak in observations in 1979 compared to models in 1976–77 may be due to the models picking up the observed regime shift 1976–77 in the Pacific Ocean as a contemporaneous increase in warming. With weak El Niños affecting observations during 1977–1980 (Wolter and Timlin, 2011), this may not have shown up in observed temperature records until 1979–80. To explain differences between models and observations requires further investigation of the relationship between identifiable regime shifts and step-like increases in temperature. For example, as a hydrodynamic phenomenon, a regime shift may change the energy balance of a region, but a warming (cooling) response may feature in temperature statistics as an unusually warm (cool) event a few years either side of the change.

Relationship between 'hiatus' periods, shifts and warming trends

Fifty-eight models in the RCP4.5 MME undergo significant step changes (p<0.01) in 1996–98, so are treated as statistical analogues of the observed shift in 1997. The size of each shift, the following shift, years between shifts, the internal trend and equilibrium climate sensitivity (ECS) were all tested for correlation (Table 1). The

1996–98 shift size is correlated with the length of the following interval (0.50, p<0.01; Figure 2a), the preceding interval (0.33, p<0.01) and the size of the next shift (0.43, p<0.01) but not with trend magnitude (0.06, NS) or ECS (0.14, NS, Figure 2c). Trend size showed an inverse relationship with its duration (-0.34, p~0.01; Figure 2b) associating longer intervals with lower trends. Trend lengths varied between 7 and 26 years, compared to the current length of 18 years Figure 2d). ECS is correlated with the following shift size (0.57, p<0.01), but not with the intervening trend (-0.13, NS). Of the 58 internal trends, 13 are non-significant (NS), 11 were p<0.05, 10 p<0.01 and 24 p<0.001. For the five observed post-1996 trends, three are non-significant and two are p<0.05 (Jones and Ricketts, 2015). Observations are at the lower end of the sample in Figures 2a, b and d, but are well within statistical limits, especially if the differences in coverage and representation between observations and models are taken into account (which would lead to a slightly higher internal trend in the observations) (Schmidt et al., 2014;Cowtan et al., 2015;Karl et al., 2015).

Table 1. Correlation matrix between variables associated with models that shift 1996–98 (n=58) that include the size of that shift and the next shift, the period length between shifts, the period length prior, the period trend, the likelihood of the null hypothesis for that trend and ECS (n=54). Correlation significance is defined not significant (NS, greyed), p<0.05 (*, standard) and p<0.01 (**, bold). Significance and correlation values are mirrored across the table.

	96–98 shift (°C)	Next shift (°C)	Period length (y)	Period prior (y)	Period trend	Trend $p\|H_0$	ECS
96–98 shift (°C)		**	**	*	NS	MS	NS
Next shift (°C)	**0.43**		*	NS	NS	NS	**
Period length (y)	**0.50**	0.33		NS	**	*	NS
Period prior (y)	0.33	0.11	0.15		NS	NS	NS
Period trend	0.06	0.15	**-0.34**	0.26		*	NS
Trend $P\|H_0$	-0.18	0.01	-0.29	-0.17	-0.51		NS
ECS	0.14	**0.57**	0.13	-0.26	-0.13	0.21	

Expanding the sampling period to 1996–2005, 101 of the 107 members of the RCP4.5 MME undergo at least one step change, but the correlation between step size and ECS remains non-significant (0.19, NS; Table 2). However, for the following interval (2006–15) the correlation rises to 0.68 and varies between 0.57 and 0.82 for subsequent decadal periods to 2095. For the preceding decades, the correlation between ECS and step size is 0.41 for 1976–85 and 0.49 for 1986–95 (both p<0.01). The low correlation between ECS and step size in 1996–2005 may be due to a rebound from the negative forcing of the Mt Pinatubo eruption in the models, which has been over-estimated by about one third (Schmidt et al., 2014). In 1956–65, where aerosols from the 1963 Mt Agung eruption produce downwards shifts in a few models, the correlation between the size of the shift and ECS is negative (-0.52, p<0.01), reflecting a strong model response to volcanic aerosol loading.

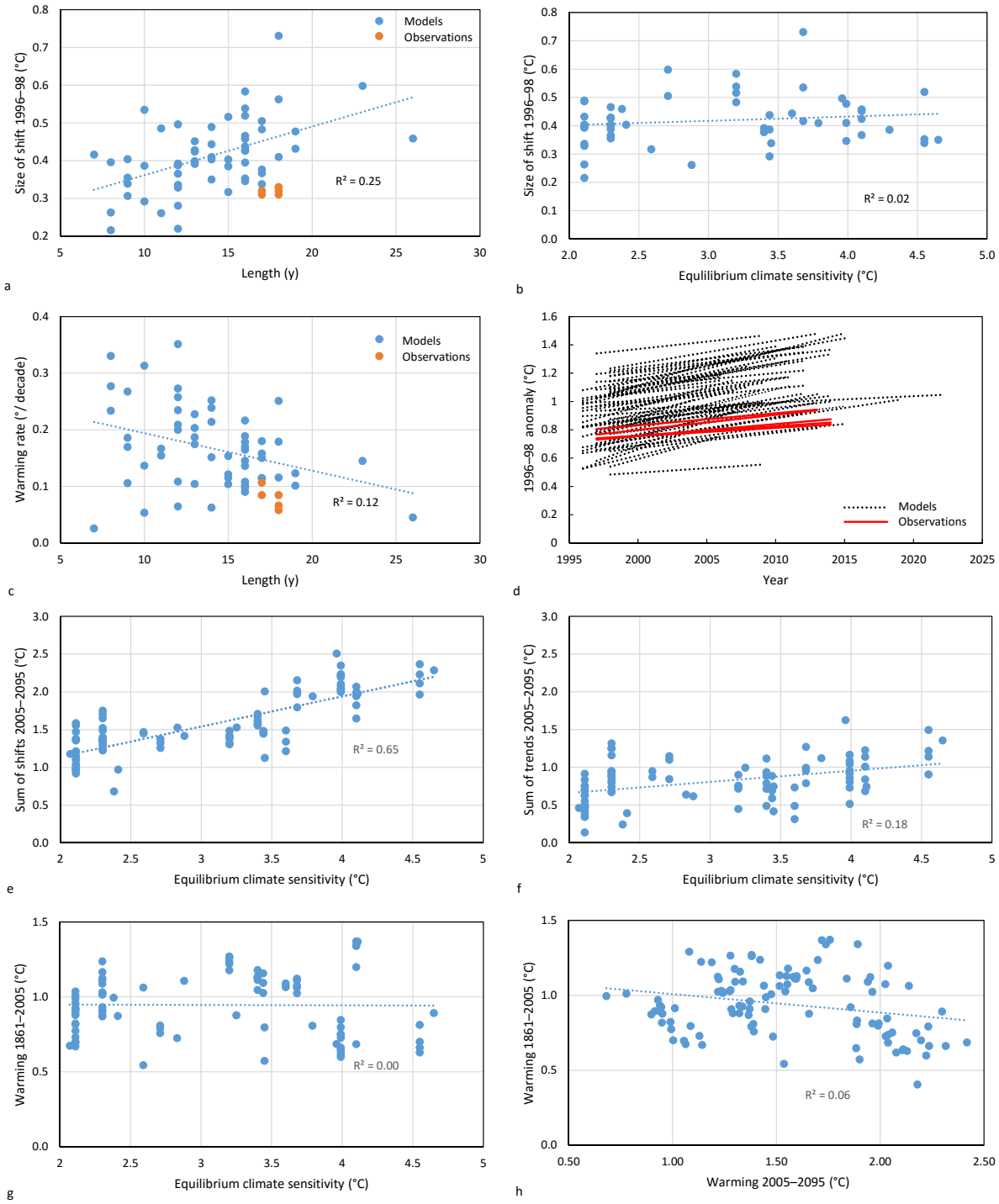

Figure 2. Multi-model ensemble (RCP4.5, 107 members) characteristics of historical (1861–2005), 'hiatus' and forced (2006–2095) periods. 2a) relationship between the 1996–98 step changes and following period length, b) with model equilibrium climate sensitivity (ECS) and c) between the 'hiatus' warming rate and length. 2d) Internal trends and lengths for the 58 'hiatus' events identified in 1996–98. 2e) Total shifts 2006–2095 and ECS, f) total internal trends, 2006–2095 and ECS, 2g) total warming 1861–2005 and ECS, h) total warming 1861–2005 and 2006–2095.

The period of forcing (2006–2095) in the RCP4.5 MME was analysed for total shifts and total internal trends. Note that according to the bivariate test, total shifts are largely inclusive of internal trends because the test assumes that the change at time T_{i0} is completely step-like (see Supplementary Information JR2015). These totals were compared with each model's ECS and total warming 2006–95 based on difference between five-

year averages centred on 2006 and 2095. Correlations between total shifts with total warming 2006–95 and ECS are both 0.81 (p<0.01; Table 2). The MME averages for total shifts and total warming are 1.57°C and 1.55°C, respectively. Total internal trends 2006–2095 average 0.81°C, and correlate with ECS (0.43, p<0.01) at a rate lower than for steps. Applying linear regression, 66% of the variance of total warming over the 21st century (2006–95) with ECS can be explained by step changes in temperature (Figure 2e), whereas the sum of internal trends can only explain 18% of that variance (Figure 2f). Steps measured as total warming minus internal trends 2006–95 correlate with ECS almost as highly as total shifts (0.72, p<0.01). Therefore, for the RCP4.5 MME, step changes represent about 3.5 times more of intermodel variance than trends. Shifts in temperature therefore dominate the warming process over decadal timescales in the climate models.

Table 2. Shifts collated according to decades from 1876 to 2195 from the RCP4.5 MME, showing shifts up and down with the magnitude of the shift correlated with ECS and its significance. Also shown are the correlations between total warming, shifts and trends over the observed and simulated periods and ECS. Correlation significance is defined not significant (NS, greyed), p<0.05 (*, standard) and p<0.01 (**, bold). Total ensemble correlations are n=107 and ensemble ECS correlations are n=92.

Period	Shifts up	Shifts down	Correlation with ECS	Significance
Shifts 1876–1885	0	26	-0.40	*
Shifts 1886–1895	13	1	-0.32	NS
Shifts 1896–1905	7	1	-0.09	NS
Shifts 1906–1915	31	0	0.27	NS
Shifts 1916–1925	65	0	0.27	*
Shifts 1926–1935	17	1	0.09	NS
Shifts 1936–1945	33	0	0.20	NS
Shifts 1946–1955	6	1	-0.85	*
Shifts 1956–1965	4	12	-0.52	*
Shifts 1966–1975	29	0	0.33	NS
Shifts 1976–1985	56	0	0.41	**
Shifts 1986–1995	34	0	0.49	**
Shifts 1996–2005	101	0	0.19	NS
Shifts 2006–2015	83	0	0.68	**
Shifts 2016–2025	82	0	0.65	**
Shifts 2026–2035	70	0	0.74	**
Shifts 2036–2045	82	0	0.66	**
Shifts 2045–2055	75	0	0.57	**
Shifts 2056–2065	65	0	0.67	**
Shifts 2066–2075	61	0	0.60	**
Shifts 2076–2085	51	0	0.66	**
Shifts 2086–2095	27	0	0.82	**
Warming 1860–2005			-0.01	NS
Warming 2006–2095			0.81	**
Shifts 1860–2005			-0.01	NS
Shifts 2006–2095			0.81	**
Trends 1860–2005			-0.09	NS
Trends 2006–2095			0.42	**

For the observational period simulations (1861–2005), total shifts and total internal trends correlate poorly with ECS (-0.01 and -0.09, both NS, Table 2). Simulated historical warming (the 2000–05 average minus the 1861–99 average) is negatively correlated with 21st century warming (2006–95, -0.25, p~0.01). Historical observations to date are therefore unlikely to be able to provide useful information about ECS and potential 21st century warming. This is despite shifts dominating internal trends in 20th century warming in both models and observations.

Even though many shifts over the 20th century in the MME correlate significantly with model ECS, neither the 1996–05 period, or total warming over the 20th century correlate with either ECS (Figure 2g) or the 21st century warming in the RCP4.5 MME (Figure 2h). The lack of predictability in the 20th century may in part be due to negative volcanic forcing counteracting the warming response in the more sensitive models, removing the influence of ECS on the results. The combination of both positive and negative forcings over the 20th century seems to be enough to cancel out any relationship between ECS and shift magnitude. The implication of this finding is that the magnitude of 20th century warming is not a reliable guide to potential future risk.

21st Century simulations

The four emissions pathways, RCP2.6, 4.5, 6 and 8.5 cover a wide range of forcing to 2100. Figures 1c–f show the percentage of step changes in any given year for the multi-model ensemble for each of these pathways. For RCP2.6, peaks in shift frequency occur to about 2050, after which the ensemble reaches stabilisation and some models step downward, the earliest in 2051. The RCP4.5 ensemble produces frequent shifts that peak around 2025 and decline towards the end of the century. RCP6 produces a fairly constant rate of shifts and RCP 8.5 produces sustained shifts throughout the century, peaking in the 2080s at a higher rate than 1996–98. Simulated global mean warming undergoes step-like changes throughout the 20th century, then changes into a step and trend process as forcing increases. The result is a step-ladder like process that changes in to an elevator-like process. These changes are illustrated using two types of chart: one shows the temperature anomaly with steps dividing internal trends (Figure 2a) and the other shows the T_{i0} statistic for a forty-year moving window through each time series (Figure 2b–e). The HadGEM2-ES single model ensemble is used to illustrate these (Figure 2).

This ensemble simulation shares the same historical forcing to 2005. This particular simulation warms by less than observations to 2010, with a reversal 1964–1980, then warms substantially in a series of steps over the next few decades. It undergoes a shift of 0.37±0.01°C in 1998, one year after the observed shift. The next shift occurs in 2012, 2013, 2014 and 2015 in the four simulations, ranging from 0.40°C to 0.49°C in absolute terms and 0.19°C to 0.27°C measured from the end of the pre-shift trend to the start of the post-shift trend. The first half of the 21st century shows the influence of decadal variability on mediating step changes (Figure 3a). In 2021, the RCP2.6 simulation undergoes a shift and is higher than the others for most of that decade. The RCP6.0 simulation is lower than the others from 2025–45 before accelerating under a sustained step-and-trend process.

In Figure 2b–e, successive horizontal lines extending right from low Ti_0 values indicate step-ladder-like behaviour. Horizontal lines that stay on the right at high T_{i0} values indicate both step-like and trending behaviour. A 'cloud' to the far right, as in Figure 2e, shows a trend-dominated process. Summarising 21st century behaviour under increasing emissions, RCP2.6 shows a return to step-like changes, stabilising around 2050, RCP4.5 shows a return to step-like change late century, RCP6.0 shows increasing trend-like behaviour and RCP8.5 shows a consistent trend to the end of the 21st century. The cloud in figure 2e we interpret as numerous regional step-like changes, integrating into a curve at the global scale. The bivariate test becomes less reliable under these conditions because of the presence of highly-autocorrelated data (see Supplementary Information JR2015 (Jones and Ricketts, 2015)). A similar situation exists for sea level rise data, where individual tide gauge records exhibit step ladder-like behaviour at individual locations and global mean sea level forms a curve at the global scale (Jones et al., 2013).

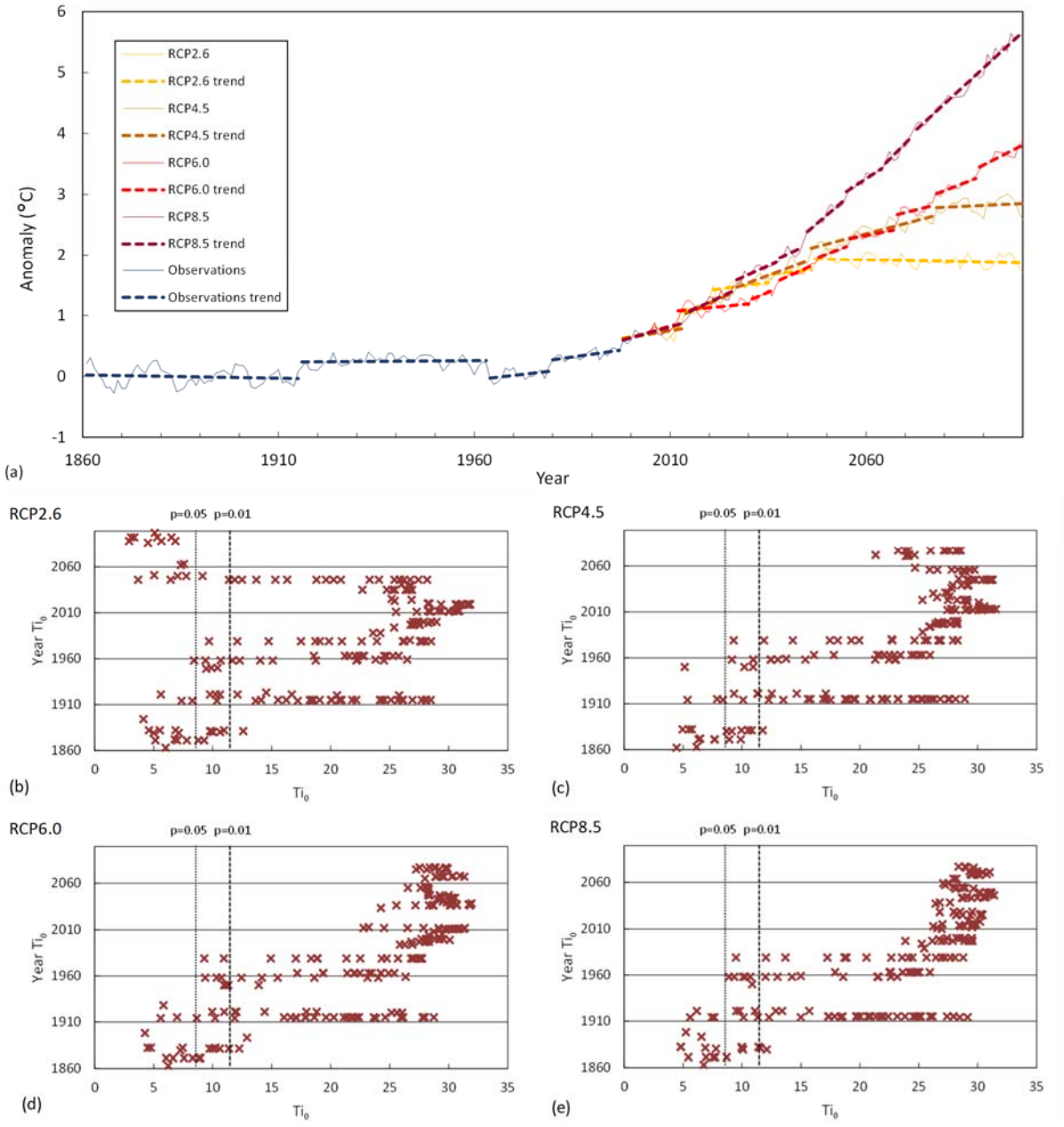

Figure 3. Global mean surface temperature as analysed by the multi-step bivariate test. 2a) Step and trend breakdown of global means surface temperature in the RCP2.6, 4.5, 6.5 and 8.0 simulations from the HadGEM-ES model. 2 b–e) T_{i0} results from a 40-year moving window for the RCP2.6, 4.5, 6.5 and 8.0 simulations, respectively.

Potential for stabilisation

The 61 RCP2.6 simulations were analysed to determine the relationship between stabilisation and ECS. The last step change in each member of this MME occurs between 2018 and 2092, with 48 being positive and 13 negative. This timing is weakly correlated with ECS (0.18, NS) and there are no significant correlations between the size of the last shift, or to the gradient of the following trend, which are roughly 50% positive/negative. Forty-six trends are NS, 12 at $p>0.05$ and 3 at $p<0.01$. The effect of strong reductions in greenhouse gas emissions therefore stabilises global mean temperature by preventing positive step changes and reducing trends to a minimum. However, the temperature at which the climate stabilises (2081–2100 average) is influenced by model ECS, with a correlation of 0.61 ($p<0.01$).

The lack of a clear relationship between climate sensitivity and stabilisation, suggests that factors influencing climate variability, most likely decadal variability, are contributing to its timing. Although the models do not contain all the mechanisms that simulate long-term climate risk, such as dynamic ice-sheet processes, these results suggest that stabilisation of climate during this century is a realistic ambition for climate policy. For the higher emission scenarios, stabilisation cannot occur until much later in the century (RCP4.5) or beyond. However, the significant correlation between the temperature of stabilisation and ECS confirms that emissions reductions can be effective in limiting warming, but this analysis shows that other factors affect its timing.

Discussion

The analysis undertaken by JR2015 for observations (Jones and Ricketts, 2015) is repeated here for simulated global mean temperature from the CMIP3 and CMIP5 archives. As for observations, shifts dominate trends. Total warming for 1861–1899 to 2000–2005 across the MME averages 1.01°C and internal trends 1861–2005 average 0.42°C. For observations, internal trends averaged 0.34°C 1880–2013/14 and total warming 0.87°C from a baseline of 1880–1899 to 2010–2014. Internal trends account for about 40% of warming in both data sets. Warming is therefore dominated by shifts in both observed and simulated global mean warming over the 20th century. This result is largely independent of the slightly different baselines.

Collectively, the MME of 20th century climate reproduces the major shifts seen in observations. Fifty-five percent of the 107-member ensemble from CMIP5 undergo a step change in 1996–98, 40% in 1976–78 and 19% in 1986–88, the main peaks in the second half of the 20th century. The other main patterns of the 20th century: the quiescent period mid-century and shifts in the early part of the century are also reproduced, but less well. We therefore have confidence in the models' representation of non-linear behaviour, where shifts dominate the global warming process over decadal timescales. The exact nature of the mechanisms contributing to these shifts needs further work.

An ongoing controversy is whether the recent period starting in mid-1997 is a short-term deviation from a long-term trend or a specific phenomenon in its own right (Boykoff, 2014;Lewandowsky et al., 2015;Trenberth, 2015;Lewandowsky et al., 2016). Because this period is being used to claim that global warming is not happening or poses less of a risk than projected by the IPCC (Boykoff, 2014), efforts are being made to either defend the trend and show that a hiatus does not exist (Cahill et al., 2015;Karl et al., 2015;Rajaratnam et al., 2015), or to explain the processes causing it (Kosaka and Xie, 2013;Meehl et al., 2013a;England et al., 2014;Watanabe et al., 2014;Yao et al., 2015). Here, we conclude that so-called hiatus periods are a normal part of climate behaviour, where stable regimes are punctuated by shifts in climate, consistent with the suggestion by Franzke (2014).

Investigation of the 'hiatus' period detects step changes during 1996–98 in 58 out of 107 independent model runs. The observed interval is 18 years in length, while in this sample, the longest period is 26 years and eight models have 18-year or longer intervals. The size of these shifts do not correlate with the trend of the following period nor with ECS. Furthermore, there is no correlation between ECS and shift size over the decade 1996–2005 or for total simulated warming over the historical period to 2005. The latter is also slightly negatively correlated (-0.26, P~0.01) with total warming 2006–2095 in the RCP4.5 MME, suggesting that past warming is no guide to future warming and may even be misleading. This correlation may be due to positive (greenhouse gas) and negative (aerosols, volcanoes) 20th century forcings cancelling each other out between models of varying climate sensitivity. This will factor into observations. The possible over-estimation of negative forcing in the models (Santer et al., 2014;Schmidt et al., 2014) may bias the model results, but will not be enough to radically change these findings.

Further analysis of steps and internal trends in the RCP4.5 MME suggest that 66% of the intermodel variance of total warming in the 21st century with ECS (2006–95) can be explained by shifts, whereas internal trends over the same period only explain 18% of the variance. This is a ratio of 3.7. Even if trends are subtracted from shifts, the most conservative assumption within a nonlinear framing, the ratio is 2.7. There is no substantial

relationship between ECS and total warming, step changes or internal trends over the period 1861–2005, implying that observed warming to date does not act as a good predictor for potential future warming. Warming follows a step-ladder like process to the end of the 20th century, when it moves into a step and trend, or elevator-like process. The time it remains elevator-like depends strongly on the strength of net radiative forcing. RCP2.6 simulations stabilise between 2018 and 2092 whereas step change in RCP8.5 increase in frequency over the century. Warming in this MME becomes dominated by trends rather than steps, which we interpret as an increase in entropy causing many local shifts in temperature, much like a boiling pot. In the RCP2.6 simulations, many models stabilise temperatures by mid-century. However, given the world is tracking at higher emissions, stabilisation of global surface temperature would require a more rapid peak and decline that in RCP2.6.

Conclusions

When both observed and simulated temperatures are analysed for shifts against a stationary reference, they show that over decadal timescales, step changes dominate the warming process. The dates of shifts coinciding with well-documented regime changes, nominate *H2*, where external forcing and internal variability are interacting to produce nonlinear change, as the more likely explanation for how climate changes, over *H1*. This does not disprove climate being quasi-linear over longer timescales (justifying the use of trend analysis over longer periods) but does question the use of trend analysis for assessing near-term (decadal scale) climate risk. When shifts in simulated temperature are analysed first, they explain approximately three times the intermodel variance as internal trends.

These findings have fundamental implications for how a changing climate should be analysed and communicated for decision making. Climate shifts affect systems as shocks and can rapidly change the incidence of extreme events, leading to critical thresholds being breached unexpectedly. Changes at the global scale in the order of 0.3°C can be associated with changes in the order of 0.7–0.8 °C in some locations (Jones, 2012;Jones and Ricketts, 2015), leading to considerable changes in local climate risk (Jones et al., 2013). The finding that step changes dominate the warming process on decadal time scales, means that how climate is analysed and communicated to manage climate risk, needs to be comprehensively re-thought.

Supplementary information

Method

The structure and application of the bivariate test used in this paper is described in the companion paper JR2015 and its supporting information. For each time series of mean annual simulated surface temperature, a series of significantly significant step changes ($p<0.01$) is produced. Depending on the time series, one or more stable configurations will result and the most stable is selected, the one with fewest members if two are produced with the same frequency. Weaknesses of the bivariate test are described in the discussion below. The result is a sequence of dates in a time series. The intervening trends are then also calculated using ordinary least squares analysis producing a record of step and trends for each time series. Five multi-model ensembles from the CMIP3 (1) and CMIP5 (4) archives were then available for further analysis. Most analysis undertaken was correlation analysis, both in Microsoft Excel and Python, cross-checked to ensure consistency.

Data

Data used are simulated annual mean surface temperature from the Climate Model Intercomparison Project (CMIP)3 and CMIP5 archives.

CMIP3/AR4

Data were downloaded under script control 17 July 2014. Data were also reloaded and cross checked from the KNMI data explorer web site on 25 Feb 2015 as per the CMIP5 data below. In all, 102 model runs were downloaded, with 14 being ensembles, and the rest being independent runs.

Within the metadata for each file are model name and identifiers, which are either run<N> or E<L> where L is the list of run numbers in an ensemble average. The models, their forcing, and run and ensemble numbers are listed in Supplementary Table 1.

Models were forced by observed natural and anthropogenic factors to 2000 or 2001, and by SRES scenarios A1b or A2 through to 2099 or 2100. The BCC model is an exception, being forced by the SRESA2 scenario from 1871.

Supplementary Table 1. List of modelling groups and global climate models used for simulations of 20th and 21st century climate, available from the CMIP3 database managed by PCMDI http://www-pcmdi.llnl.gov/ipcc/info_for_analysts.php. The forcing factors for 20th century climate are: G – Well-mixed greenhouse gases, O – Ozone, SD – Sulfate direct, SI – Sulfate indirect, BC – Black carbon, OC – Organic carbon, MD – Mineral dust, SS – Sea salt, LU – Land use, SO – Solar irradiance and V – Volcanic aerosol. Updated from (CSIRO and BoM, 2007).

Originating Group(s), Country	Model	Forcings used in model simulations	Scenarios	Runs & (E)nsembles	Start date
Bjerknes Centre for Climate Research, Norway	BCCR	G, SD	SRESA1b	1	1850
Beijing Climate Center, China	BCC	G, SD*	SRESA2	1	1871
Canadian Climate Centre, Canada	CCCMA T47	G, SD	SRESA1b	1–5, E1–3	1850
			SRESA2	1	1850
Canadian Climate Centre, Canada	CCCMA T63	G, SD	SRESA1b	1	1850
Meteo-France, France	CNRM	G, O, SD, BC	SRESA1b	1	1860
			SRESA2	1	1860
CSIRO, Australia	CSIRO-MK3.0	G, O, SD	SRESA1b	1	1871
			SRESA2	1	1871
CSIRO, Australia	CSIRO-MK3.5	G, O, SD	SRESA1b	1	1871
			SRESA2	1	1871
Geophysical Fluid Dynamics Lab, USA	GFDL 2.0	G, O, SD, BC, OC, LU, SO, V	SRESA1b	1	1861
			SRESA2	1	1861
Geophysical Fluid Dynamics Lab, USA	GFDL 2.1	G, O, SD, BC, OC, LU, SO, V	SRESA1b	1	1861
			SRESA2	1	1861
NASA/Goddard Institute for Space Studies, USA	GISS-AOM	G, SD, SS	SRESA1b	1–2, E1–2	1850
NASA/Goddard Institute for Space Studies, USA	GISS-E-H	G, O, SD, SI, BC, OC, MD, SS, LU, SO, V	SRESA1b	1–3, E1–3	1880
NASA/Goddard Institute for Space Studies, USA	GISS-E-R	G, O, SD, SI, BC, OC, MD, SS, LU, SO, V	SRESA1b	1–4, E1–4	1880
			SRESA2	1	1880
Instituto Nazionale di Geofisica e Vulcanologia, Italy	INGV	G, SD	SRESA1b	1	1870
			SRESA2	1	1870
LASG/Institute of Atmospheric Physics, China	IAP	G, SD	SRESA1b	1–3, E1–3	1850
Institute of Numerical Mathematics, Russia	INMCM	G, SD, SO	SRESA1b	1	1871
			SRESA2	1	1871
Institut Pierre Simon Laplace, France	IPSL	G, SD, SI	SRESA1b	1	1860
			SRESA2	1	1860
Centre for Climate Research, Japan	MIROC-H	G, O, SD, BC, OC, MD, SS, LU, SO, V	SRESA1b	1–3, E1–3	1850
			SRESA2	1–3, E1–3	1850
Centre for Climate Research, Japan	MIROC-M	G, O, SD, BC, OC, MD, SS, LU, SO, V	SRESA1b	1	1900
Meteorological Institute University of Bonn, Meteorological Research Institute KMA, Germany/Korea	MIUB	G, SD, SI	SRESA1b	1–3, E1–3	1860
			SRESA2	1–3, E1–3	1860
	MPI-ECHAM5	G, O, SD, SI	SRESA1b	1–4, E1–3	1860

Max Planck Institute for Meteorology DKRZ, Germany			SRESA2	1–3, E1–3	1860
Meteorological Research Institute, Japan	MRI	G, SD ,SO	SRESA1b	1–5, E1–5	1851
			SRESA2	1–5, E1–5	1851
National Center for Atmospheric Research, USA	NCAR-CCSM	G, O, SD, BC, OC, SO, U	SRESA1b	1–4,9, E1–2	1870
			SRESA2	1–4	1870
National Center for Atmospheric Research, USA	NCAR-PCM1	G, O, SD, SO, V	SRESA1b	1,4	1890
			SRESA2	1–4, E2–4	1890
Hadley Centre, UK	HADCM3	G, O, SD, SI	SRESA1b	1	1860
			SRESA2	1	1860
Hadley Centre, UK	HADGEM1	G, O, SD, SI, BC, OC, LU, SO, V	SRESA1b	1	1860
			SRESA2	1	1860

CMIP5/AR5

Data were downloaded from the KNMI data explorer web site http://climexp.knmi.nl/ RCP4.5, RCP6.0 and RCP8.5 (7 Jan 2015), RCP2.6 (19 Feb 2015). Files were renamed under script control using metadata within the files (see below) to simplify later handling.
Four multi-model ensembles were analysed: RCP2.6 (61 members), RCP4.5 (107 members), RCP6.0 (47 members) and RCP8.5 (80 members). Details are listed in Table SI2.

Supplementary Table 2. List of modelling groups and global climate models used for simulations of 20th and 21st century climate, available from the CMIP5 database http://cmip-pcmdi.llnl.gov/cmip5/availability.html, with run numbers (r(N)) and physics perturbations (p(L)), and equilibrium climate sensitivity (ECS). ECS is taken from Sherwood et al. (2014) unless otherwise noted. If not allocated otherwise, runs have the physical perturbation p1.

Centre	Model	RCP2.6	RCP4.5	RCP6.0	RCP8.5	ECS
BoM/CSIRO, Australia	ACCESS1-0		r1		r1	3.79
BoM/CSIRO, Australia	ACCESS1-3		r1		r1	3.45
Beijing Climate Center, China	BCC-CSM1-1	r1	r1	r1	r1	2.88
Beijing Climate Center, China	BCC-CSM1-1-M	r1	r1	r1		
Beijing Normal University, China	BNU-ESM	r1	r1		r1	4.11
Canadian Climate Centre, Canada	CanESM2	r1–5	r1–5		r1–5	3.68
National Center for Atmospheric Research, USA	CCSM4	r1,3–6	r1–6	r1–6	r1–6	3.20[1]
National Center for Atmospheric Research, USA	CESM1-BGC		r1		r1	
National Center for Atmospheric Research, USA	CESM1-CAM5	r1–3	r1–3	r1–3	r1–2	4.10[2]
Euro-Mediterranean Center on Climate Change, Italy	CMCC-CM		r1		r1	
Euro-Mediterranean Center on Climate Change, Italy	CMCC-CMS		r1		r1	
Meteo-France, France	CNRM-CM5	r1	r1		r1,2,4,6,10	3.25
CSIRO/QCCCE, Australia	CSIRO-Mk3-6-0	r1–10	r1–10	r1–10	r1–10	3.99
EC-Earth Consortium	EC-EARTH	r8,12	r1,2,6,8,9,12		r1,2,8,9,11,12,13	3.4[3]
LASG/Institute of Atmospheric Physics, China	FGOALS-g2	r1	r1		r1	3.45

The First Institute of Oceanography, SOA, China	FIO-ESM		r1–3	r1–3	r1–3	
Geophysical Fluid Dynamics Lab, USA	GFDL-CM3		r1	r1	r1	3.96
Geophysical Fluid Dynamics Lab, USA	GFDL-ESM2G		r1	r1	r1	2.38
Geophysical Fluid Dynamics Lab, USA	GFDL-ESM2M		r1		r1	2.41
NASA/Goddard Institute for Space Studies, USA	GISS-E2-H	r1p1–r1p3	r1p1–r5p3	r1p1–r1p3	r1p1–r1p3	2.30
NASA/Goddard Institute for Space Studies, USA	GISS-E2-H-CC		r1			
NASA/Goddard Institute for Space Studies, USA	GISS-E2-R	r1p1–r1p3	r1p1–r5p3	r1p2,r1p3	r1p1–r1p3	2.11
NASA/Goddard Institute for Space Studies, USA	GISS-E2-R-CC		r1			
National Institute of Meteorological Research, South Korea	HadGEM2-AO	r1	r1	r1	r1	
Met Office Hadley Centre, UK	HadGEM2-CC		r1		r1	
Met Office Hadley Centre, UK	HadGEM2-ES	r1–4	r1–4	R2–4	r1–4	4.55
Institute of Numerical Mathematics, Russia	INM-CM4		r1		r1	2.07
Institut Pierre Simon Laplace, France	IPSL-CM5A-LR	r1–4	r1–4	r1	r1–4	4.1
Institut Pierre Simon Laplace, France	IPSL-CM5A-MR	r1	r1	r1	r1	
Institut Pierre Simon Laplace, France	IPSL-CM5B-LR		r1		r1	2.59
Centre for Climate Research, Japan	MIROC5	r1–3	r1–3	r1–3	r1–3	2.71
Centre for Climate Research, Japan	MIROC-ESM	r1	r1	r1	r1	4.65
Centre for Climate Research, Japan	MIROC-ESM-CHEM	r1	r1	r1	r1	
Max Planck Institute for Meteorology DKRZ, Germany	MPI-ESM-LR	r1–3	r1–3		r1–3	3.60
Max Planck Institute for Meteorology DKRZ, Germany	MPI-ESM-MR	r1	r1–3		r1	3.44
Meteorological Research Institute, Japan	MRI-CGCM3	r1	r1	r1	r1	2.59
Norwegian Climate Center, Norway	NorESM1-M	r1	r1	r1	r1	2.83
Norwegian Climate Center, Norway	NorESM1-ME	r1	r1	r1	r1	

[1.] The estimate from the model developers(Meehl et al., 2011) is preferred.
[2.] Estimate from the model developers(Meehl et al., 2013b)
[3.] Estimate from the model developers(Lacagnina et al., 2014)

Discussion of results

The bivariate test is one of the most robust tests available for testing serially independent time series data for step, or abrupt, changes. However, climate data fulfils this condition only some of the time. The evidence presented in JR2015, supports previous conclusions that annual time series of observed temperature can be regarded as serially independent, especially where it shows little or limited sign of intervening trends that are statistically significant. Qualitatively, this is the step ladder-like behaviour where large step changes occur in a

time series with limited internal trends. For the 20th century simulations to 2005 analysed here, these same conditions are considered to be met. A longer discussion on the reliability of the test under these conditions can be found in the SI for JR2015.

Where there is the potential for steps and trends to be present in the same time series, then the bivariate test, and all other tests used in assessing step changes, become less robust. These conditions are present in most simulations after 2005. This is the principal reason for developing the rule-based test with multiple iterations to assess stable configurations.

Some testing was carried out with artificial time series containing red noise (autocorrelation 0.1 with a one-year lag, 0.25 with a seven-year lag) combined with random step changes and trends. By itself, red noise will produce step changes at a higher rate than serially independent data, thereby overstating the probability of exceedance. However, in using the test for detection, we are mainly interested in using the test to detect the timing and magnitude of steps as accurately as possible.

Our major assumption about a warming climate is that regime shifts (an organised and abrupt change in the structure and function of a system), red-noise driven shifts in the variable under analysis, random shifts and trending behaviour are all possible. In such a system, abrupt changes will become more common, therefore increase relative risk if those changes are driving impacts. This is the main purpose for the bivariate test in this paper, where it is being used to detect large shifts in mean temperature.

When all these phenomena are combined in artificial data, the combination of steps, red noise, random noise and trends will detect step changes that:

1. May not be serially independent, therefore overstating the probability of being a clear step change but not its timing or magnitude,
2. May produce a step change that averages two underlying step changes (this has also been noted with observations),
3. May variously suppress or amplify potential step changes, thus affecting the drivers of risk,
4. May detect a step change in a trending variable, where the internal steps by themselves may be insignificant.

The latter possibility, we consider as the only real false positive, but all the others warrant caution. Points one and two will reveal step changes, but not necessarily their case, point three suggests that not all underlying changes in a system may manifest and point four illustrates where the test will falsely identify steps and trends. The latter can be identified visually, by measuring the end-to-start distance between internal trends across the change point and visually as per Figure 3 in the paper. In terms of risk, for mean global surface warming, this situation is associated with the high radiative forcing, so may register a false positive for an independent step change, but not for rapid changes in risk.

References

Boykoff, M.T., 2014: Media discourse on the climate slowdown. *Nature Climate Change*, **4**, 156-158.

Bücher, A. and J. Dessens, 1991: Secular trend of surface temperature at an elevated observatory in the Pyrenees. *Journal of Climate*, **4**, 859-868.

Buishand, T., 1984: Tests for detecting a shift in the mean of hydrological time series. *Journal of Hydrology*, **73**, 51-69.

Cahill, N., S. Rahmstorf and A.C. Parnell, 2015: Change points of global temperature. *Environmental Research Letters*, **10**, 084002.

Corti, S., F. Molteni and T.N. Palmer, 1999: Signature of recent climate change in frequencies of natural atmospheric circulation regimes. *Nature*, **398**, 799-802.

Cowtan, K., Z. Hausfather, E. Hawkins, P. Jacobs, M.E. Mann, S.K. Miller, B.A. Steinman, M.B. Stolpe and R.G. Way, 2015: Robust comparison of climate models with observations using blended land air and ocean sea surface temperatures. *Geophysical Research Letters*, **42**, 2015GL064888.

CSIRO and BoM, 2007: *Climate Change in Australia: technical report 2007*. CSIRO, Melbournepp.

England, M.H., S. McGregor, P. Spence, G.A. Meehl, A. Timmermann, W. Cai, A.S. Gupta, M.J. McPhaden, A. Purich and A. Santoso, 2014: Recent intensification of wind-driven circulation in the Pacific and the ongoing warming hiatus. *Nature Climate Change*, **4**, 222-227.

Franzke, C.L.E., 2014: Warming trends: Nonlinear climate change. *Nature Climate Change*, **4**, 423-424.

Gan, T.Y., 1995: Trends in air temperature and precipitation for Canada and north-eastern USA. *International Journal of Climatology*, **15**, 1115-1134.

Hasselmann, K., 2002: Is Climate Predictable? In: *The Science of Disasters: Climate Disruptions, Heart Attacks, and Market Crashes* [Bunde, A., J. Kropp and H.J. Schellnhuber (eds.)] Springer, Berlin Heidelberg, 141-188.

Hegerl, G. and F. Zwiers, 2011: Use of models in detection and attribution of climate change. *Wiley Interdisciplinary Reviews: Climate Change*, **2**, 570-591.

Jones, R.N., 2012: Detecting and attributing nonlinear anthropogenic regional warming in southeastern Australia. *Journal of Geophysical Research*, **117**, D04105.

Jones, R.N., C.K. Young, J. Handmer, A. Keating, G.D. Mekala and P. Sheehan, 2013: *Valuing Adaptation under Rapid Change*. National Climate Change Adaptation Research Facility, Gold Coast, Australia, 182 pp.

Jones, R.N. and J.H. Ricketts, 2015: *Analysing steps in global and regional observed air temperature*. Climate Change Working Paper No. 34, Victoria Institute of Strategic Economic Studies, Victoria University, Melbourne, 20 pp.

Karl, T.R., A. Arguez, B. Huang, J.H. Lawrimore, J.R. McMahon, M.J. Menne, T.C. Peterson, R.S. Vose and H.-M. Zhang, 2015: Possible artifacts of data biases in the recent global surface warming hiatus. *Science*, **348**, 1469-1472.

Kirono, D. and R. Jones, 2007: A bivariate test for detecting inhomogeneities in pan evaporation time series. *Australian Meteorological Magazine*, **56**, 93-103.

Kirtman, B., S. Power, A.J. Adedoyin, G. Boer, R. Bojariu, I. Camilloni, F. Doblas-Reyes, A. Fiore, M. Kimoto, G. Meehl, M. Prather, A. Sarr, C. Schär, R. Sutton, G.J.v. Oldenborgh, G. Vecchi and H.-J. Wang, 2013: Near-term Climate Change: Projections and Predictability. In: *Climate Change 2013: The Physical Science Basis. Working Group I contribution to the IPCC 5th Assessment Report* [Stocker, T.F., D. Qin, G.-K. Plattner, M. Tignor, S.K. Allen, J. Boschung, A. Nauels, Y. Xia, V. Bex and P.M. Midgley (eds.)] Cambridge University Press, Cambridge and New York, 121.

Kosaka, Y. and S.-P. Xie, 2013: Recent global-warming hiatus tied to equatorial Pacific surface cooling. *Nature*, **501**, 403-407.

Lacagnina, C., F. Selten and A.P. Siebesma, 2014: Impact of changes in the formulation of cloud-related processes on model biases and climate feedbacks. *Journal of Advances in Modeling Earth Systems*, **6**, 1224-1243.

Lewandowsky, S., N. Oreskes, J.S. Risbey, B.R. Newell and M. Smithson, 2015: Seepage: Climate change denial and its effect on the scientific community. *Global Environmental Change*, **33**, 1-13.

Lewandowsky, S., J.S. Risbey and N. Oreskes, 2016: The “Pause” in Global Warming: Turning a Routine Fluctuation into a Problem for Science. *Bulletin of the American Meteorological Society*, **97**, 723–733.

Maronna, R. and V.J. Yohai, 1978: A bivariate test for the detection of a systematic change in mean. *Journal of the American Statistical Association*, **73**, 640-645.

Meehl, G.A., W.M. Washington, J.M. Arblaster, A. Hu, H. Teng, C. Tebaldi, B.N. Sanderson, J.-F. Lamarque, A. Conley, W.G. Strand and J.B. White, 2011: Climate System Response to External Forcings and Climate Change Projections in CCSM4. *Journal of Climate*, **25**, 3661-3683.

Meehl, G.A., A. Hu, J.M. Arblaster, J. Fasullo and K.E. Trenberth, 2013a: Externally Forced and Internally Generated Decadal Climate Variability Associated with the Interdecadal Pacific Oscillation. *Journal of Climate*, **26**, 7298-7310.

Meehl, G.A., W.M. Washington, J.M. Arblaster, A. Hu, H. Teng, J.E. Kay, A. Gettelman, D.M. Lawrence, B.M. Sanderson and W.G. Strand, 2013b: Climate Change Projections in CESM1(CAM5) Compared to CCSM4. *Journal of Climate*, **26**, 6287-6308.

North, G.R., K.-Y. Kim, S.S.P. Shen and J.W. Hardin, 1995: Detection of Forced Climate Signals. Part 1: Filter Theory. *Journal of Climate*, **8**, 401-408.

Overland, J., S. Rodionov, S. Minobe and N. Bond, 2008: North Pacific regime shifts: Definitions, issues and recent transitions. *Progress In Oceanography*, **77**, 92-102.

Potter, K., 1981: Illustration of a new test for detecting a shift in mean in precipitation series. *Monthly Weather Review*, **109**, 2040-2045.

Rahmstorf, S., G. Foster and A. Cazenave, 2012: Comparing climate projections to observations up to 2011. *Environmental Research Letters*, **7**, 044035.

Rajaratnam, B., J. Romano, M. Tsiang and N. Diffenbaugh, 2015: Debunking the climate hiatus. *Climatic Change*, **133**, 129–140.

Reeves, J., J. Chen, X.L. Wang, R. Lund and Q.Q. Lu, 2007: A Review and Comparison of Changepoint Detection Techniques for Climate Data. *Journal of Applied Meteorology and Climatology*, **46**, 900-915.

Rodionov, S.N., 2005: A brief overview of the regime shift detection methods. *Large-Scale Disturbances (Regime Shifts) and Recovery in Aquatic Ecosystems: Challenges for Management Toward Sustainability. UNESCO-ROSTE/BAS Workshop on Regime Shifts*, *Varna, Bulgaria*, Velikova, V. and N. Chipev, Eds., City, pp 17-24.

Sahin, S. and H.K. Cigizoglu, 2010: Homogeneity analysis of Turkish meteorological data set. *Hydrological Processes*, **24**, 981-992.

Santer, B.D., C. Mears, C. Doutriaux, P. Caldwell, P.J. Gleckler, T.M.L. Wigley, S. Solomon, N.P. Gillett, D. Ivanova, T.R. Karl, J.R. Lanzante, G.A. Meehl, P.A. Stott, K.E. Taylor, P.W. Thorne, M.F. Wehner and F.J. Wentz, 2011: Separating signal and noise in atmospheric temperature changes: The importance of timescale. *Journal of Geophysical Research*, **116**, D22105.

Santer, B.D., C. Bonfils, J.F. Painter, M.D. Zelinka, C. Mears, S. Solomon, G.A. Schmidt, J.C. Fyfe, J.N.S. Cole, L. Nazarenko, K.E. Taylor and F.J. Wentz, 2014: Volcanic contribution to decadal changes in tropospheric temperature. *Nature Geoscience*, **7**, 185-189.

Schmidt, G.A., D.T. Shindell and K. Tsigaridis, 2014: Reconciling warming trends. *Nature Geoscience*, **7**, 158-160.

Solomon, A., L. Goddard, A. Kumar, J. Carton, C. Deser, I. Fukumori, A.M. Greene, G. Hegerl, B. Kirtman, Y. Kushnir, M. Newman, D. Smith, D. Vimont, T. Delworth, G.A. Meehl and T. Stockdale, 2011: Distinguishing the Roles of Natural and Anthropogenically Forced Decadal Climate Variability. *Bulletin of the American Meteorological Society*, **92**, 141-156.

Swanson, K.L., G. Sugihara and A.A. Tsonis, 2009: Long-term natural variability and 20th century climate change. *Proceedings of the National Academy of Sciences*, **106**, 16120-16123.

Trenberth, K.E., 2015: Has there been a hiatus? *Science*, **349**, 691-692.

Vivès, B. and R.N. Jones, 2005: *Detection of Abrupt Changes in Australian Decadal Rainfall (1890-1989)*. CSIRO Atmospheric Research Technical Paper, CSIRO Atmospheric Research, Melbourne, 54 pp.

Watanabe, M., H. Shiogama, H. Tatebe, M. Hayashi, M. Ishii and M. Kimoto, 2014: Contribution of natural decadal variability to global warming acceleration and hiatus. *Nature Climate Change*.

Wolter, K. and M.S. Timlin, 2011: El Niño/Southern Oscillation behaviour since 1871 as diagnosed in an extended multivariate ENSO index (MEI.ext). *International Journal of Climatology*, **31**, 1074-1087.

Yao, S.-L., G. Huang, R.-G. Wu and X. Qu, 2015: The global warming hiatus—a natural product of interactions of a secular warming trend and a multi-decadal oscillation. *Theoretical and Applied Climatology*, 1-12.

Zhou, J. and K.-K. Tung, 2013: Deducing Multidecadal Anthropogenic Global Warming Trends Using Multiple Regression Analysis. *Journal of the Atmospheric Sciences*, **70**, 3-8.